MEASURING THE NONLINEAR PERFORMANCE OF INDIUM GALLIUM PHOSPHIDE USING THE Z-SCAN AND INTENSITY VARIATION METHODS

THESIS

Jacob A. Wilson
AFIT-ENP-MS-17-J-013

DEPARTMENT OF THE AIR FORCE
AIR UNIVERSITY

AIR FORCE INSTITUTE OF TECHNOLOGY

Wright-Patterson Air Force Base, Ohio

DISTRIBUTION STATEMENT A.
APPROVED FOR PUBLIC RELEASE; DISTRIBUTION UNLIMITED.

AFIT-ENP-MS-17-J-013

MEASURING THE NONLINEAR PERFORMANCE OF INDIUM GALLIUM PHOSPHIDE USING THE Z-SCAN AND INTENSITY VARIATION METHODS

THESIS

Presented to the Faculty

Department of Engineering and Physics

Graduate School of Engineering and Management

Air Force Institute of Technology

Air University

Air Education and Training Command

In Partial Fulfillment of the Requirements for the

Degree of Master of Science in Optical Sciences & Engineering

Jacob A. Wilson

June 2017

AFIT-ENP-MS-17-J-013

MEASURING THE NONLINEAR PERFORMANCE OF INDIUM GALLIUM PHOSPHIDE USING THE Z-SCAN AND INTENSITY VARIATION METHODS

Jacob A. Wilson, BS

Committee Membership:

Dr. Michael A. Marciniak
Chair

Dr. Mitchell B. Haeri
Member

Dr. Shekhar Guha
Member

Maj. Manuel R. Ferdinandus
Member

AFIT-ENP-MS-17-J-013

Abstract

Due to the increasing complexity of electronic and optical applications, there is a strong need for more customization of nonlinear materials. This thesis investigates the nonlinear performance on the tunable semiconductor, indium gallium phosphide. Indium gallium phosphide's band-gap can be customized as it is a tunable material compared to most nonlinear materials, which have fixed band-gaps. The nonlinear characteristics of indium gallium phosphide are unknown, so the well-researched nonlinear material indium phosphide is used as a comparison. Research performed in this document demonstrates two common methods that determine the nonlinear properties of a material. These methods include the Z-scan and an intensity variation scan. Indium phosphide shows expected nonlinear behavior, which verifies the methodology used in the research. Indium gallium phosphide also shows signs of nonlinear behavior. Discussion in the report provides a comparison of the nonlinear performance of the two materials, and provides insight on future experimentation on indium gallium phosphide.

Acknowledgments

I would like to thank Dr. Michael Marciniak and Dr. Mitch Haeri for giving me this amazing opportunity. They are two of the best advisors I have ever had, and also two of the most professional people I have ever encountered. I could not be more grateful for all of their guidance and support throughout this project.

I would also like to thank Dr. Shekhar Guha and Jonathan Slagle. They both provided so much physical insight and encouragement for this project. Even though I did my work in California, they were always readily available from Ohio to give me new perspectives and to answer my questions.

I would also like to thank Mike Ehritz and Janes Henry from Raytheon. Mike Ehritz helped me tremendously in getting familiar with new equipment in the lab and James Henry made the onboarding process at Raytheon go so smoothly. Also, special thanks to my family for their encouragement throughout the graduate program at AFIT. Especially my grandpa (Opa), who has always given me confidence to reach for the stars in my career of science.

Finally, I would like to thank Raytheon and the Air Force Research Laboratory for supporting this research.

Jacob A. Wilson

Table of Contents

List of Figures

MEASURING THE NONLINEAR PERFORMANCE OF INDIUM GALIUM PHOSPHIDE USING THE Z-SCAN AND INTENSITY VARIATION METHODS

I. Introduction

General Issue

The nonlinear optical properties of semiconductors have been experimentally studied with high intensity lasers for various optical device applications since the invention of the laser in the 1960s. Some of these applications include optical switching [1], holography [2], laser frequency tuning by optical parametric oscillation [3], and commercial solid state lasers [4]. Accurately modelling the nonlinear performance of semiconductor based devices requires knowledge of the nonlinear material coefficients. Some of the important nonlinear material parameters are the carrier absorption coefficients and refractive index cross sections, carrier recombination times, and the two-photon absorption coefficients. This thesis discusses the nonlinear performance of the semiconductors, indium phosphide (InP) and indium gallium phosphide (InGaP). The purpose of this research effort is to show that InGaP exhibits nonlinear properties. InGaP has a tunable band-gap, so there are many more electronic and optical applications compared to most nonlinear materials that have that a fixed band-gap. Indium phosphide is used as a "gold standard" for nonlinear behaviour due to it having well-researched nonlinear properties. Since the nonlinear properties of InP are well understood, the material is used to validate the experimental setup and results of InGaP.

When considering the nonlinear performance of a material, two of the properties that are of particular interest are the material's nonlinear absorption coefficient and its nonlinear index of refraction. Both of these parameters change the intensity of the light in a nonlinear way as the light transverses through the medium. By measuring these parameters, it is possible to identify how efficient a semiconductor behaves as a nonlinear material. Figure 1 below shows a representation of the output irradiance as a function of input irradiance for a linear and nonlinear material.

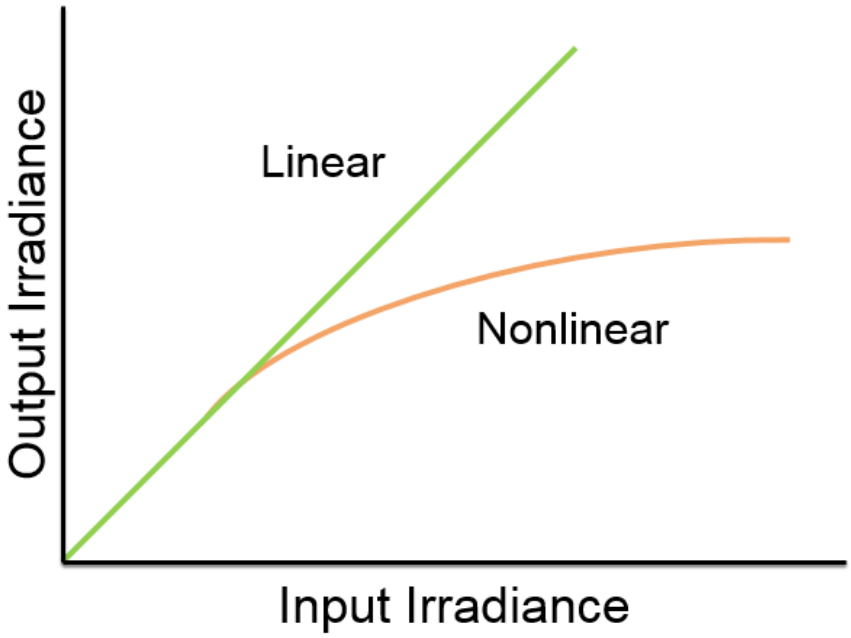

Figure 1. Linear and nonlinear behavior for increasing input irradiance

A major process that defines the nonlinear performance of a semiconductor is nonlinear absorption, as this process best attenuates a laser beam. Nonlinear absorption includes multiphoton absorption such as two-photon absorption, which is when two photons are simultaneously absorbed and excite the atom into a higher-lying state. The two-photon process is initiated by the electric field of the laser light. Two-photon absorption generates free carriers which can have multiple effects on the incident laser

beam. First, the free carriers in the conduction band absorb light through free carrier absorption. Next, the carriers refract and absorb light through plasma and band filling effects [5]. The heat generated by the laser pulse can also change the refractive index of the semiconductor at mid-gap wavelengths.

Two-photon absorption was first observed in cadmium sulphide in 1964 [6]. Since then, two-photon absorption has been studied in many different materials, particularly in semiconductors. Two-photon materials can be divided into binary and ternary compounds. The binary compounds operate over a fixed spectral band. InP is an example of a binary compound as it has a direct band-gap. InGaP is a ternary compound, so it has a tunable band-gap. By adjusting the stoichiometry, the band-gap of ternary compounds can be tuned across spectrums of interest. This is a useful capability because it allows more customization of the material for various electronic and optical applications. Two-photon semiconductor materials work well against short laser pulses (femtoseconds to nanosecond), since the two photon process is initiated by the electric field of the laser beam.

This report determines if InGaP has viable nonlinear performance. To the best of my knowledge, the nonlinear behavior of InGaP as not been determined to date. If InGaP has adequate nonlinear performance, it has to have a sufficient two photon coefficient. In a material with strong nonlinear absorption, the output intensity eventually approaches a constant value beyond a certain input intensity. A comparison study was done in this report with InP. InP is considered a “gold standard” in terms of nonlinear materials due to its highly researched nonlinear effects including its strong two photon absorption [7]. Since InP has known nonlinear properties, a comparison study shows validation of the

experimental methods and the results of InGaP. If the results for InGaP are promising, more studies can be performed to determine more information on its nonlinear behavior.

The methods used to examine the nonlinear properties of InP and InGaP were the Z-scan and intensity variation (also known as I-Scan) techniques. Both of these methods are useful in determining the nonlinear performance of a material. The Z-scan technique [8,9] allows for measurements of optical nonlinearities by a simple transmission experiment, while the I-scan [10] keeps the sample fixed and the input energy is varied. The I-scan method is particularly useful because a two-photon absorption coefficient can be extracted from the data, which is important for understanding the nonlinear performance of a material.

Thesis Organization

This document describes the research and development of finding the nonlinear behavior of the semiconductor InGaP. Chapter 2 provides background information on the nonlinear properties and applications of the materials InP and InGaP. This begins with how light interacts with matter, and the derivation of the nonlinear wave equation is included. Nonlinear behavior in semiconductors is described along with a derivation for a theoretical value of the two-photon coefficient. Chapter 3 provides the methodology of this report, the Z-scan and I-scan experiments. It covers the properties of the materials tested along with the detector and laser used in the set-ups. Chapter 4 addresses results for the nonlinear properties of InGaP. It includes the results for InP, which is tested because it has known nonlinear behavior. A comparison of the nonlinear behavior in InP and in InGaP is also shown. Chapter 5 provides a conclusion, remarks and suggestions for future work.

II. Literature Review

Chapter Overview

This chapter provides an overview of the physics and mathematics on which this research is based. A background on the primary topics consists of nonlinear light-matter interactions, nonlinear absorption in semiconductors, and the I-scan and Z-scan experiment. Relevant citations have been provided to supplement a given discussion or offer a resource for a more detailed development of a specific topic.

Nonlinear Light-Matter Interactions

To describe any light-matter interaction, it is standard to begin with Maxwell's equations:

$$\nabla \times \mathrm{H} = \frac{\partial D}{\partial t}, \tag{1}$$

$$\nabla \cdot \mathrm{D} = 0, \tag{2}$$

$$\nabla \times \mathrm{E} = -\frac{\partial B}{\partial t}, \tag{3}$$

$$\nabla \cdot B = 0, \tag{4}$$

In these equations, it is assumed that the surface charge density σ and the volume charge density ρ are both zero. Also, the magnetic flux density B and the magnetic field H are related through $\mathrm{B} = \mu_0 \mathrm{H}$, where μ_0 is the permeability of free space. The electric field E is related to the electric flux density D through $\mathrm{D(E)} = \epsilon_0 \mathrm{E} + \mathrm{P(E)}$, where ϵ_0 is the

permittivity of free space and the dielectric polarization P(E) is the dipole moment per unit volume.

To describe nonlinear light-matter interactions, it is necessary rewrite Maxwell's equations with the nonlinear polarization term, P_{NL}, which can be written as:

$$\nabla \times \mathrm{H} = \frac{\partial}{\partial t}(\epsilon_0 \epsilon_1 \mathrm{E} + \mathrm{P_{NL}}) = \epsilon_0 \epsilon_1 \frac{\partial E}{\partial t} + \frac{\partial \mathrm{P_{NL}}}{\partial t}, \tag{5}$$

$$\nabla \times \mathrm{E} = -\frac{\partial}{\partial t}(\mu_0 \mathrm{H}) = -\mu_0 \frac{\partial \mathrm{H}}{\partial t}, \tag{6}$$

where Equation 5 and Equation 6 are a coupled set of differential equations, and in order to extract the nonlinear wave equation, the rotation of Equation 6 is considered:

$$\nabla \times \nabla \times \mathrm{E} = \nabla \times (\mu_0 \frac{\partial \mathrm{H}}{\partial t}) = -\mu_0 \frac{\partial}{\partial t}(\nabla \times \mathrm{H}). \tag{7}$$

Substituting Equation 5 into Equation 7 yields:

$$\nabla \times \nabla \times \mathrm{E} = -\mu_0 \frac{\partial}{\partial t}(\epsilon_0 \epsilon_1 \frac{\partial E}{\partial t} + \frac{\partial \mathrm{P_{NL}}}{\partial t}). \tag{8}$$

Equation 8 can then be rewritten with a general identity:

$$\nabla(\nabla \cdot \mathrm{E}) - \nabla^2 \mathrm{E} = -\mu_0 \frac{\partial}{\partial t}(\epsilon_0 \epsilon_1 \frac{\partial E}{\partial t} + \frac{\partial \mathrm{P_{NL}}}{\partial t}). \tag{9}$$

Due to only transverse fields being considered ($\nabla \cdot \mathrm{E} = 0$), Equation 9 can be simplified:

$$\nabla^2 \mathrm{E} = \mu_0 \frac{\partial}{\partial t}(\epsilon_0 \epsilon_1 \frac{\partial E}{\partial t} + \frac{\partial \mathrm{P_{NL}}}{\partial t}). \tag{10}$$

With the fact that $\epsilon_0 \mu_0 = c^{-2}$, where c is the speed of light in vacuum, Equation 10 can be rearranged and simplified as:

$$\nabla^2 \mathrm{E} - \epsilon_0 \epsilon_1 \frac{\partial E}{\partial t} = \frac{1}{c^2} \frac{\partial^2 \mathrm{P_{NL}}}{\partial t^2}. \tag{11}$$

This is known as the nonlinear inhomogeneous wave equation [11]. Solving the nonlinear wave equation assumes the solution consists of a linear summation of plane waves with discrete frequency components. The frequency is ω_j and the wave vector is $k_j = \frac{n_j \omega_j}{c}$, where n_j is the refractive index. By definition, plane waves only propagate along the z-axis, and the solutions can be described by:

$$E(z,t) = \frac{1}{2}\left(\sum_{j=1}^{N} E_j(z,t) e^{i(k_j z - \omega_j t)}\right). \tag{12}$$

Similarly, the nonlinear polarization can be written as:

$$P(z,t) = \frac{1}{2}\left(\sum_{j=1}^{N} P_j(z,t) e^{i\omega_j t}\right). \tag{13}$$

Taking the second-order spatial derivative of the electric field and the second-order temporal derivative of both the electric field and nonlinear polarization yields:

$$\frac{\partial^2}{\partial z^2} E(z,t) = \frac{1}{2}\sum_{j=1}^{N}\left(\frac{\partial^2 E_j}{\partial z^2} + 2ik_j \frac{\partial E_j}{\partial z} - k_j^2 E_j\right) e^{ik_j z} e^{-i\omega_j t}, \tag{14}$$

$$\frac{\partial^2}{\partial t^2} E(z,t) = \frac{1}{2}\sum_{j=1}^{N}\left(\frac{\partial^2 E_j}{\partial t^2} - 2i\omega_j \frac{\partial E_j}{\partial t} - \omega_j^2 E_j\right) e^{ik_j z} e^{-i\omega_j t}, \tag{15}$$

$$\frac{\partial^2}{\partial t^2} P_{NL}(z,t) = \frac{1}{2}\sum_{j=1}^{N}\left(\frac{\partial^2 P_{NL_j}}{\partial t^2} - 2i\omega_j \frac{\partial P_{NL_j}}{\partial t} - \omega_j^2 P_{NL_j}\right) e^{-i\omega_j t}. \tag{16}$$

With the electric field and induced nonlinear polarization field, and assuming that the amplitude changes slowly compared to the frequency of the plane wave, the following assumptions can be made:

$$\frac{\partial^2 E_j}{\partial t^2} \ll \omega_j \frac{\partial E_j}{\partial t} \ll \omega_j^2 E_j, \tag{17}$$

$$\frac{\partial^2 E_j}{\partial z^2} \ll k_j \frac{\partial E_j}{\partial z} \ll k_j^2 E_j, \tag{18}$$

$$\frac{\partial^2 P_{NL_j}}{\partial t^2} \ll \omega_j \frac{\partial P_{NL_j}}{\partial t} \ll \omega_j^2 P_{NL_j}. \tag{19}$$

These assumptions are known as the "slowly varying envelope approximation." The second-order spatial and temporal derivatives of the amplitude of the electric field and the first and second-order temporal derivatives of the nonlinear polarization can be neglected under the assumption [12]. Using these assumptions, Equations 14, 15, and 16, and combining them with the nonlinear inhomogeneous wave equation (Equation 11) yields:

$$\begin{aligned} \frac{1}{2}\sum_{j=1}^{N}\left(2ik_j\frac{\partial E_j}{\partial z} - k_j^2 E_j - \frac{\epsilon_j}{c^2}\left[2i\omega_j\frac{\partial E_j}{\partial t} - \omega_j^2 E_j\right]\right)e^{i(k_j z - \omega_j t)} \\ = \frac{1}{2}\frac{1}{c^2\epsilon_0}\sum_{j=1}^{N}\left(-\omega_j^2 P_{NL_j}\right)e^{-i\omega_j t}. \end{aligned} \tag{20}$$

Because $k_j^2 = \frac{\epsilon_j \omega_j^2}{c^2}$, the equation can be simplified:

$$\sum_{j=1}^{N}\left(2ik_j\frac{\partial E_j}{\partial z} + 2i\frac{\epsilon_j}{c^2}\omega_j^2\frac{\partial E_j}{\partial t}\right)e^{ik_j z} = \frac{-1}{c^2\epsilon_0}\sum_{j=1}^{N}\omega_j^2 P_{NL_j}. \tag{21}$$

This equation holds true for each of the frequency components. Since $n_j = \sqrt{\epsilon_j}$ and $k_j = \frac{n_j \omega_j}{c}$, the equation can be reduced to:

$$\frac{\partial E_j}{\partial z} + \frac{n_j}{c}\frac{\partial E_j}{\partial t} = i\frac{\omega_j}{c n_j}\frac{1}{2\epsilon_0} P_{NL_j} e^{-ik_j z}. \tag{22}$$

Equation 22 is the well-known nonlinear wave equation. It provides the foundation for describing all nonlinear light-matter interactions, including nonlinear absorption.

Nonlinear Behavior in Semiconductors

When light travels through a transparent material, it can affect the properties of the material at high intensities. Eventually the output intensity will not be linear with the input intensity. An example of this is when the intensity is high enough, it can cause the refractive index of the material to change. This is an example of nonlinear behavior. There are a few ways nonlinear behavior can happen in semiconductors, including nonlinear absorption and free-carrier absorption and refraction.

Ordinary linear absorption in semiconductors may be described as a one-step process (one-photon), whereby an electron is photo-excited from the valence band to the conduction band, absorbing one photon of energy $\hbar\omega$. The absorption is described by an absorption coefficient α, such that

$$\frac{dI}{dz} = -\alpha I, \tag{23}$$

where I is the optical intensity (power per unit area) of the pulse and z is the sample depth.

All semiconductors usually exhibit some linear absorption, which can be described as a material not being completely transparent over an optical path length at a given wavelength of light. This is due to the material transitions caused by absorptions of single photons whose energy ($\hbar\omega$) exceeds the semiconductor's band-gap energy(E_g). When the frequency obeys $\hbar\omega > E_g$, the rate of transitions is αI and non-zero. However, once the intensity of light is strong enough, the linear approximation for the absorption is no longer adequate. The transition rate acquires a term that is $\alpha I^2$and non-zero for frequencies ω such that $\hbar\omega \geq \frac{1}{2}E_g$. The following expression must be used:

$$\alpha(I) = \alpha + \beta I, \tag{24}$$

where β is the two-photon absorption (TPA) coefficient. Figure 2 compares linear absorption versus two-photon absorption.

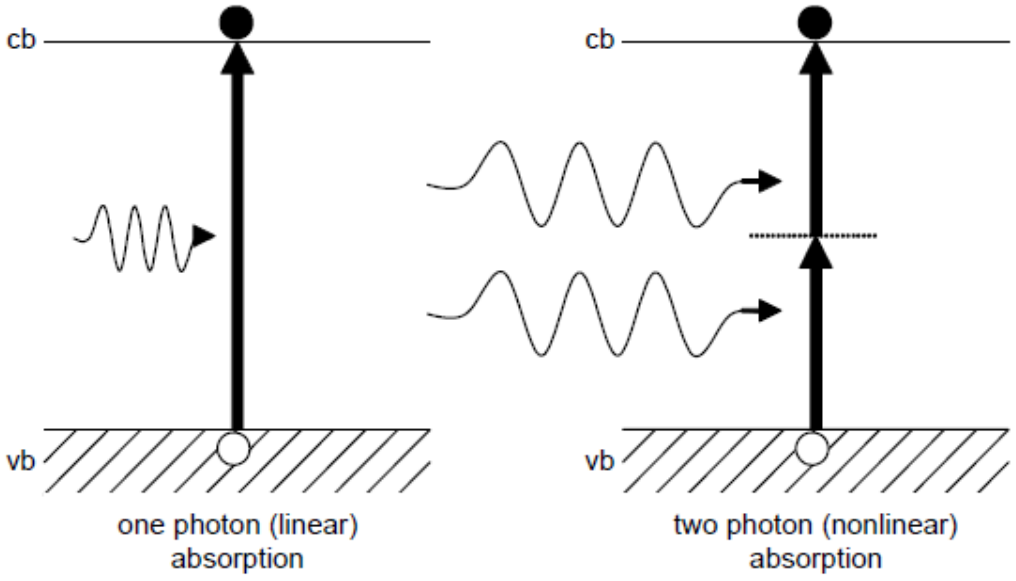

Figure 2. Diagram showing linear and nonlinear absorption of photons in a semiconductor, resulting in the generation of free carriers

Because of the band-gap between the valence and conduction bands in a semiconductor, photons can be absorbed to create an electron-hole pair. Linear absorption corresponds to one photon being absorbed to create an electron hole pair, and if more than one photon is absorbed to create the electron-hole pair, it is known as multiphoton absorption. Nonlinear absorption only occurs when there are large numbers of photons present in a short time period, which requires high intensity lasers (or pulsed lasers). Typically only 2^{nd} or 3^{rd} order nonlinear behavior can be observed in semiconductors because the strength of the optical field required to view the behavior increases with the order of the effect. Anything over the 3^{rd} order effect is rarely observed due to the substantial field size required. The most common nonlinear absorption observed is when two photons are absorbed simultaneously. This is known as two-photon absorption (TPA) [13]. The theoretical value for TPA is derived in the next section.

Two-photon Absorption

Multiphoton absorption processes have been studied for decades, beginning when they were explored by Maria Göppert-Mayer in 1931 [14]. Once the laser was invented, the multiphoton absorption processes observed by Maria Göppert-Mayer could be tested experimentally [15,16]. The main branch of theory on multiphoton absorption that has been developed after the laser invention involves the time-dependent perturbation theory.

The theory begins with the Beer-Lambert law, which relates the attenuation of light to the properties of the material through which the light is traveling. It is defined as:

$$\frac{dI}{dz} = -\sum_n \alpha_n I^n, \tag{25}$$

where α_n is the n-photon absorption coefficient and I is the irradiance in watts per square meter. The propagation direction is z. The attenuation rate of the irradiance is given by

$$\frac{dI}{dz} = -\frac{c}{\epsilon_\infty}\alpha_n I^n, \tag{26}$$

with c being the speed of light in a vacuum and ϵ_∞ is the high frequency dielectric constant of the material. The irradiance is also related to the peak electric field amplitude and the photon number density. This relation is given as

$$I = \frac{{E_0}^2(\epsilon_\infty)^{\frac{1}{2}}}{2Z_0} = \frac{c}{\sqrt{\epsilon_\infty}}\hbar\omega N_{ph}, \tag{27}$$

where E_0 is the electric field amplitude in V/m, N_{ph} is the photon number density in inverse cubic meters, and Z_0 is the vacuum impedance. The n-photon absorption process also creates N_e, which is the density of conduction electrons. This is related to the photon absorption per unit volume, given as

$$\frac{dN_{ph}}{dt} = \frac{\alpha_n}{\hbar\omega} I^n = -n\frac{dN_e}{dt}. \tag{28}$$

Finally, the n-photon absorption coefficient can be written in terms of the transition rate, W, given as

$$\alpha_n = \frac{2n\hbar\omega(2Z_0)^n W({E_0}^{2n})}{{\epsilon_\infty}^{n/2}{E_0}^{2n}}. \tag{29}$$

With time-dependent perturbation theory, the probability for an n-photon direct electron transition from an initial valence-band state v to a final conduction-band state c is given by Fermi's golden rule [17]:

$$W_n = \frac{2\pi}{\hbar}\int \left| \sum_m \sum_l \cdots \sum_j \sum_i \frac{\langle \psi_c|H|\psi_m\rangle\langle \psi_m|H|\psi_l\rangle}{[E_m - E_l - (n-1)\hbar\omega]} \right|^2 \\ \cdots \frac{\langle \psi_j|H|\psi_i\rangle}{(E_j - E_i - 2\hbar\omega)} \frac{\langle \psi_i|H|\psi_v\rangle}{(E_i - E_v - \hbar\omega)} \\ \times\ \delta[E_c(k) - E_v(k) - n\hbar\omega]\frac{d^3k}{(2\pi)^3}, \tag{30}$$

where k is the propagation vector, and $j \ldots m$ are intermediate states with energies $E_j \ldots E_m$. $E_c(k)$ and $E_v(k)$ are the energy of the valence and conduction bands in the k-space. The integration of the equation is over all values of k ranging from zero to infinity. The delta function expresses energy-conservation requirements, and the summations extend over all possible intermediate states. Next, simplifications can be made to Equation 30 depending the amount of photons being absorbed.

For the case of two-photon absorption (n=2), Equation 30 can be simplified to:

$$W_2 = \frac{2\pi}{\hbar}\int \left| \sum_i \frac{\langle \psi_c|H|\psi_i\rangle\langle \psi_i|H|\psi_v\rangle}{(E_i - E_v - \hbar\omega)} \right|^2 \times \delta[E_c(k) - E_v(k) - 2\hbar\omega]\frac{d^3k}{(2\pi)^3}. \tag{31}$$

The two-photon absorption coefficient β is related to the perturbation W_2 by:

$$\beta = \frac{2W_2(2\hbar\omega)}{I^2}. \tag{32}$$

In 1984, Wherrett [18] developed scaling rules for multiphoton interband absorption in semiconductors. He used the perturbation theory and derived a formula for direct-gap absorption coefficients based on a simplified band model. The Wherrett equation provides a universal gap dependence, and enables one to estimate absorption coefficients for a given material predicated on the known coefficients of another material. The scaling rule Wherrett developed for two-photon absorption can expressed as:

$$\beta \propto \frac{1}{{E_g}^3} \frac{(2\hbar\omega/E_g - 1)^{3/2}}{(2\hbar\omega/E_g)^5}. \tag{33}$$

This scaling rule was eventually verified experimentally by Van Stryland et al [19]. Van Stryland found the two-photon coefficient for a variety of semiconductors with different band-gaps, and confirmed the trend of a lower band-gap resulting in a higher theoretical two-photon coefficient value.

Analysis of Z-scan for a Nonlinear Medium

The Z-scan method [8,9] was developed to detect nonlinear changes in absorption and refractive index using a single light beam. Developed by Eric Van Stryland, the Z-scan method remains a standard technique for determining nonlinear optical properties of various solids and liquids. It has many advantages over other nonlinearity measurement techniques because it is simple, and gives the sign of optical nonlinearity almost immediately. The method involves translating a sample on the "z" axis (axis of propagation) through a tightly focused beam and then measuring the power transmitted through the sample. Figure 3 shows a schematic of a Z-scan experiment.

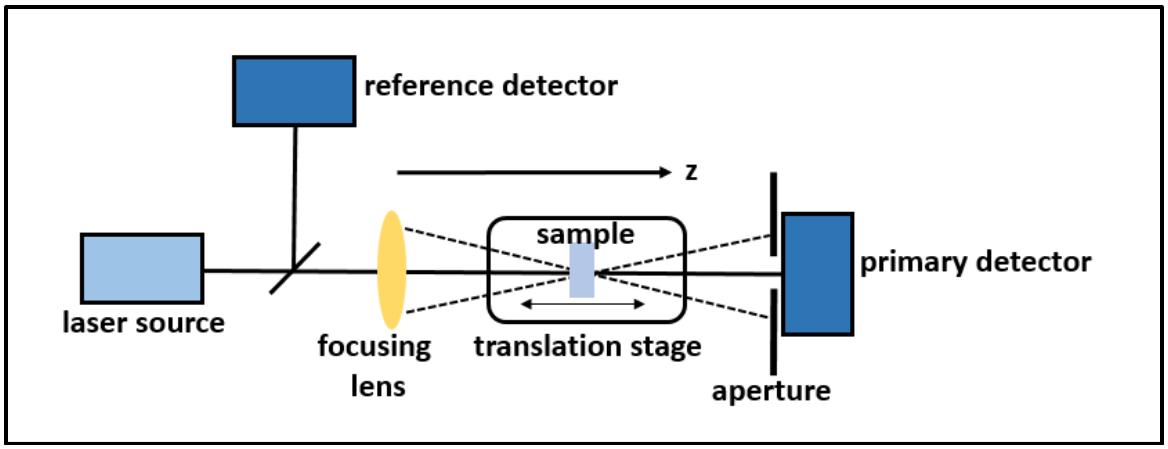

Figure 3. Diagram of Z-Scan experiment

The laser beam is focused by a lens and the sample is moved through a focal plane, where the intensity of laser light experienced by the sample is a function of the distance (z) from the focal plane to the sample. A reference detector is also placed in the setup, which monitors the input energy. An aperture is placed in front of the detector in the experimental setup and it can be opened or closed to control how much of the beam is being measured. The two configurations of the z-scan experiment are known as open and closed aperture. In an open aperture configuration, the aperture in front of the detector is opened so that it no longer impinges on the beam. The total energy of the transmitted beam is then collected. The measured transmittance is then independent of nonlinear refraction and only dependent on nonlinear absorption. In the open aperture configuration, the transmittance graph should be symmetric around the focus since the intensity distribution of a Gaussian beam is symmetric around the focus. The closed aperture configuration refers to the case where the aperture obscures the light passing through the sample. In the closed aperture configuration, effects from both nonlinear absorption and nonlinear refraction are observed. In order to distinguish between effects

due to nonlinear refraction and those due to nonlinear absorption, both open aperture and closed aperture measurements must be made. By dividing the closed-aperture scan by an open aperture scan, the effect of free-carrier absorption can be removed, giving only the effect of the nonlinear refraction [9,20].

Materials exhibit an intensity dependent absorption or refraction,

$$n(I) = n_0 + n_2 I, \tag{34}$$

where I is the incident irradiance, n_0 is the linear index of refraction, and n_2 is the nonlinear index of refraction. The transmitted intensity will change based on the nonlinearity if the sample exhibits nonlinear refraction or absorption. By monitoring the entire transmission of the sample during its scan, the dependence of absorption on the incident intensity can be found. The transmitted intensity can be defined as

$$\Delta T(z) \approx \frac{q_0}{\left[1 + \frac{Z^2}{{Z_0}^2}\right]}, \tag{35}$$

where $q_0 = \beta I_0 L_{eff}$ and Z is the sample distance away from the focal point and Z_0 is the Rayleigh range. L_{eff} is calculated using $L_{eff} = (1 - e^{-\alpha l})/\alpha$, where α is the linear absorption coefficient and l is the sample length. β is the two-photon coefficient, and I_0 is the peak irradiance illuminating the sample. For a beam of Gaussian transverse profile, the peak irradiance is defined as

$$I_0 = \frac{2 \times Pulse\ Energy}{\pi {\omega_0}^2 \tau}, \tag{36}$$

where the pulse energy is in Joules, ω_0 is the waist radius, and τ is the full width at half-maximum (FWHM) pulse duration. The spot size is calculated using $\omega_0 = 1.27\lambda f/2d$, where f is the focal length of the focusing element and d is the measured beam diameter.

For the analysis of the Z-scan experiment, it is assumed that there is a TEM_{00} Gaussian beam interacting with the sample. The electric field, $E(r,t,z)$, of Gaussian beam with a waist radius ω_0 propagating in the +z direction at a distance z from the waist, can be described as

$$E(r,t,z) = E_0(t)\frac{\omega_0}{\omega(z)}\exp\left(-\frac{r^2}{\omega^2(z)} - \frac{ikr^2}{2R(z)}\right)e^{-i\phi(z,t)}, \tag{37}$$

where $E_0(t)$ denotes the radiation electric field at the waist and r is the radial distance from the center axis of the beam. The sample introduces a phase shift $\phi(z,t)$ due to nonlinear refraction that is independent of r. $k = 2\pi/\lambda$ is the wave vector, and the beam radius $\omega(z)$ is related to the z position through

$$\omega^2(z) = {\omega_0}^2\left(1 + \frac{z^2}{{z_0}^2}\right). \tag{38}$$

The radius of curvature of the wave front at z is given as

$$R(z) = z\left(1 + \frac{{z_0}^2}{z^2}\right), \tag{39}$$

where z_0 is known as the Rayleigh range and is given by

$$Z_0 = \frac{\pi{\omega_0}^2}{\lambda}. \tag{40}$$

The Rayleigh range gives the distance over which the peak irradiance drops by one half. It is important that the sample is thinner than the Rayleigh range in order for the use of

thin-sample approximation. This means either a very thin sample or a large f-number should be used in the experiment.

Analysis of I-scan for a Nonlinear Medium

The Z-scan measures total absorption, and unless an ultra-short pulse duration (femtosecond) is used, effects of the free carriers have to be included. This makes it difficult to get a two-photon coefficient value from nanosecond pulse experiments. Another way to examine optical nonlinearities in a material is an intensity variation method known as an I-scan. This method was developed as a variant of the Z-scan method [10]. This method involves keeping the sample at a fixed location and varying the input energy instead of translating it through the focus at the same energy. The input energy can be varied using multiple attenuators in front of the focusing lens. Figure 4 below shows a standard I-scan setup.

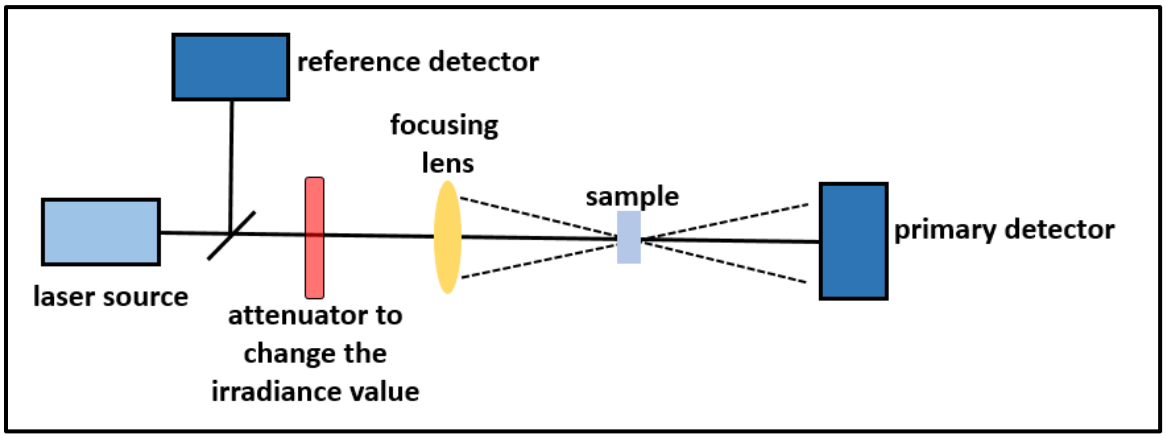

Figure 4. Diagram of the I-Scan experiment

There are several advantages using the I-scan instead of the Z-scan. One major advantage is that the sample will have the same illumined area from the laser. In the Z-scan method, the sample is moved throughout focus so the part of the material

illuminated by the laser changes due to the beam size changing. This can lead to inconsistent data for inhomogeneous samples. Along with the same area being illuminated on the material, only one z-position has to be carefully profiled which reduces some uncertainty. However, this method does require high dynamic range detection.

The I-scan method yields plots for the transmittance as a function of irradiance of a material. In general, the greater the incoming irradiance, the smaller the transmittance in the case of multiphoton absorption. Figure 5 shows theoretical transmission curves as a function of input irradiance for a 1-cm thick sample [21]. Where the top curve levels out in the lower irradiance portion of the graph reveals the linear regime of the material. At lower input irradiances, only linear mechanisms are acting on the material. The graph also shows how the higher the β value, the more nonlinear a material performs. Materials with higher β values have lower transmittance versus intensity curves, and thus require lower input energy values to show the linear portion of the graph.

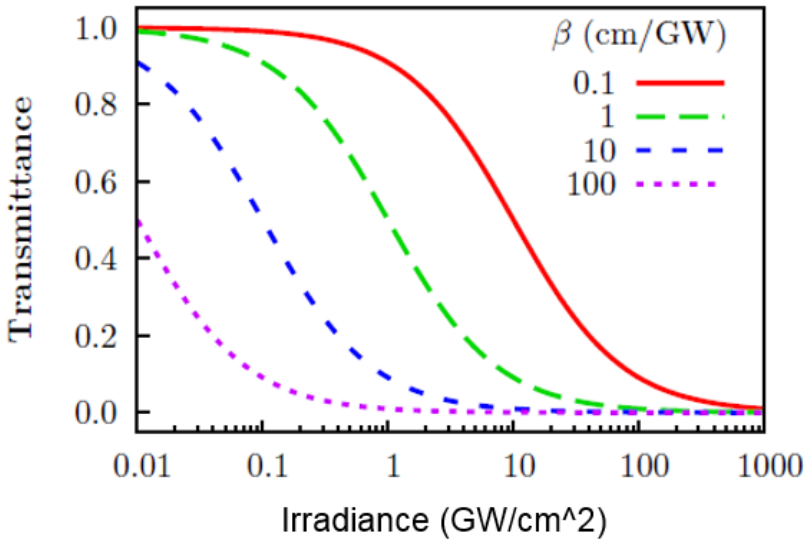

Figure 5. Theoretical transmission curves as a function of input irradiance for a 1 cm thick sample with different values of β

For a given pulse width, an input irradiance versus transmittance plot can be generated using the I-scan method. This makes it possible to estimate an effective β value for a material even if a larger pulse width is used. An effective β is the result from modeling the total non-linear absorption. The effective β includes contributions of all non-linear absorption mechanisms that become increasingly significant with more input irradiance and two-photon absorption. This makes it possible to get an estimation of β for larger pulse widths, specifically nanosecond lasers. An estimation for β can be made by extrapolating the linear fit of the effective β to zero input irradiance, which is where contributions from other non-linear mechanisms are insignificant [22].

Materials

Two materials were examined: InP and InGaP. The focus of the thesis is to demonstrate nonlinear behavior in InGaP. InP, a well characterized nonlinear material is used to compare the results of InGaP and validate the experimental set-up.

Indium Phosphide (InP)

InP was first prepared in 1910 by A. Thielf and H. Koelsch [23]. It is a binary semiconductor consisting of indium (In) and phosphorus (P) atoms in a zincblende crystal structure. At a wavelength of 1064 nm, InP has a refractive index of 3.22 and a reflectivity of 0.277 [24]. The reflectivity corresponds to the Fresnel losses of the material, and is dependent upon the indices of refraction of the material and the medium from which the light is incident upon it. The normal incidence reflectivity, R_f, is

$$R_f = \left[\frac{n_2 - n_1}{n_2 + n_1}\right]^2, \tag{41}$$

where light from a medium of index n_1 is normally incident on a medium of index n_2. The laser light comes from air (n = 1) and is normally incident on the semiconductor. The Fresnel losses are linear losses on the material, and they occur on both the incident surface and the inside surface of the material.

Much work has been done on developing InP, mainly for use in the electronics industry. Because it has a high electron velocity, it is used in high-frequency and high-power electronics. It is also used for optoelectronics devices since it has a direct bandgap of 1.344 eV. Another major use of InP is as a substrate layer for InGaAs and InGaP family of materials, which are used in photodetectors [25].

Due to all of the uses of InP, there is a lot of interest in the nonlinear behavior of the material. Most importantly, the two-photon coefficient, β. There are many recent two-photon absorption measurements, including a value of 90 cm/GW measured by Dvorak at 1064 nm with pulses of picosecond duration using the z-scan technique [26]. Earlier work with nanosecond pulses suggested a much larger coefficient in the range of 160-280 cm/GW [27]. As the pulse duration is reduced, the measured two-photon absorption values are trending towards the theoretical prediction developed by Van Stryland, which predicts values of 24 cm/GW at 1064 nm and 17 cm/GW at 1600 nm [27].

Indium Gallium Phosphide (InGaP)

InGaP is a "ternary" compound, which is composed of three different elements. It is a semiconductor composed of indium, gallium, and phosphorus. At a wavelength of 1064 nm, InGaP has a refractive index of 3.10 and a reflectivity of 0.262, which corresponds to the Fresnel losses of the material [28]. Similarly to InP, it is used in high-

power and high-frequency electronics. Some of these uses include the fabrication of high efficiency solar cells for space applications, and in high-electron-mobility transistors and heterojunction bipolar transistors [29]. Varying the stoichiometry or "x" value of a ternary material, and in this case $In_{1-x}Ga_xP$, allows one to adjust the band-gap to the desired spectrum of interest.

Summary

This chapter covered the theory on the nonlinear properties of the materials InP and InGaP. It began with how light interacts with matter, and the derivation of the nonlinear wave equation was included. The nonlinear wave equation provides the foundation for describing all nonlinear light matter interactions, including nonlinear absorption. Since InP and InGaP are both semiconductors, how nonlinear light behaves in semiconductors was explained. Next, the multiphoton absorption process known as two-photon absorption was described and the scaling rule for two-photon absorption was provided, which gives a theoretical value for the two-photon coefficient. Theory was also provided on the methodology of this report, the Z-scan and I-scan experiments. The Z-scan method is one of the most standard ways of detecting nonlinear changes in absorption. The I-scan method discussed is a variant of the Z-scan method that involves keeping the sample at a fixed location and varying the input energy instead of translating like in the Z-scan method. Finally, this chapter explained the characteristics of InP and InGaP and their applications. The next section of the report, Chapter 3, goes through the methodology of the report which was based on the theory provided in this section.

III. Methodology

Chapter Overview

This chapter provides an overview of the experiment and explains the setups which were used to show the nonlinear behavior of indium gallium phosphide (InGaP). The first setup of the experiment was a traditional open aperture Z-scan, described in Chapter 2. The Z-scan is a standard way to measure nonlinear behavior, however it is difficult to extract a two-photon coefficient (β) using a nanosecond laser. Instead of using the Z-scan technique to measure β, a standard nonlinear transmission method, known as an I-scan, also described in Chapter 2, was used. Indium phosphide (InP) was also tested in the same setups as a comparative study to InGaP due to it having known nonlinear performance. The setups showing the expected nonlinear behavior of InP help validate the nonlinear behavior of InGaP, a material that has not yet been studied for its nonlinear effects. This chapter shows pictures of both materials, explains the detectors and laser source used, and goes into the details of the Z-scan and I-scan experimental setups.

Materials Tested

The experiments tested two separate materials, InP and InGaP. Nonlinear effects on InP are well documented, but they are unknown for InGaP. Figure 6 is an image of InP and Figure 7 is an image of the InGaP sample used in the experiments.

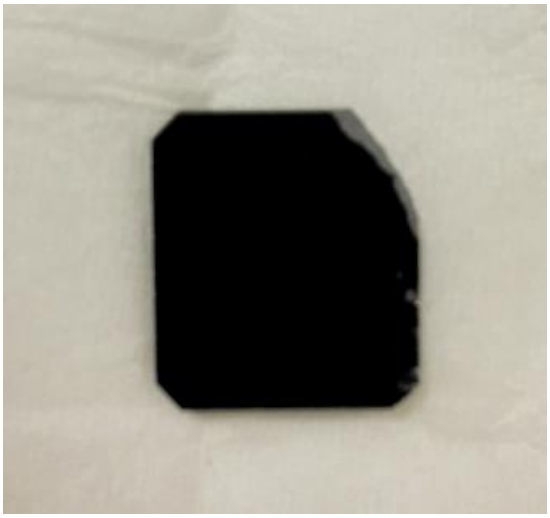

Figure 6. Visible light image of InP

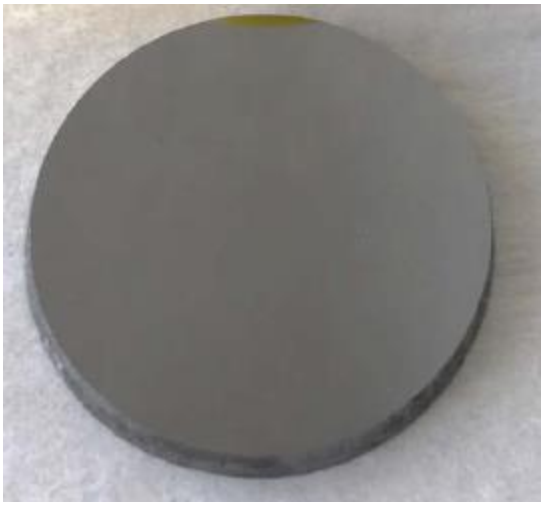

Figure 7. Visible light image of InGaP

Both of the samples were polished and uncoated. The crystal growing process of the InGaP material has not been perfected, so there is transmission non-uniformity throughout the sample. A good spot on the material was always found before taking measurements. This took some time translating the sample in the x and y positions (relative to z being laser propagation direction as described in Chapter 2) to find a spot

with high transmission. A mid-wave infrared image of the sample was taken which helped this process. This image is shown in Figure 8.

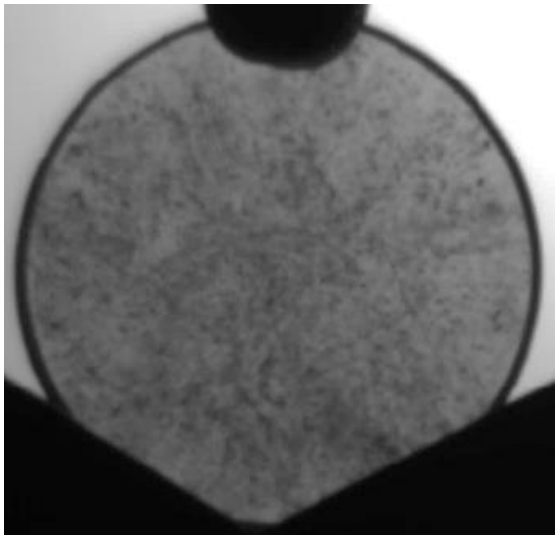

Figure 8. Mid-wave infrared image of InGaP

One of the experimental considerations was the sample thickness. The sample thickness must be less than the Rayleigh range of the focused laser beam. This is necessary for the sample to be considered thin and for the nonlinear processes to be considered to occur at a single position and not be spread across the length of the sample. The Rayleigh range was calculated by finding the beam radius at focus. The beam radius at focus was estimated by considering the F/# of the system, which is discussed in the I-scan methodology section. The InP sample thickness was 1 mm, and the InGaP sample thickness was 1.5 mm. For both materials, the Rayleigh range was 2.2 mm.

InP, being a fixed band-gap material, has a band-gap of 1.34 eV (associated with a cut-off wavelength of 0.923 μm) [24]. Indium gallium phosphide has a tunable band-gap, so one of the advantages when considering InGaP is the ability to choose a desired band-gap in the growing process. Figure 9 shows three separate samples of InGaP that

were grown to achieve the desired band-gap of 1.77 eV (0.7 μm). This was done by varying the stoichiometry or "x" value of InGaP. In this case the material has an "x" value of 0.5, giving the sample the form of $In_{0.5}Ga_{0.5}P$. Even though all of the samples were successfully grown to achieve the desired band-gap, only the B2 sample was used in the experiments. The B2 sample had the highest transmission and least amount of non-uniformity compared to the other two samples. The samples were grown by Dr. Partha Dutta, president of the United Semiconductor Limited Liability Cooperation.

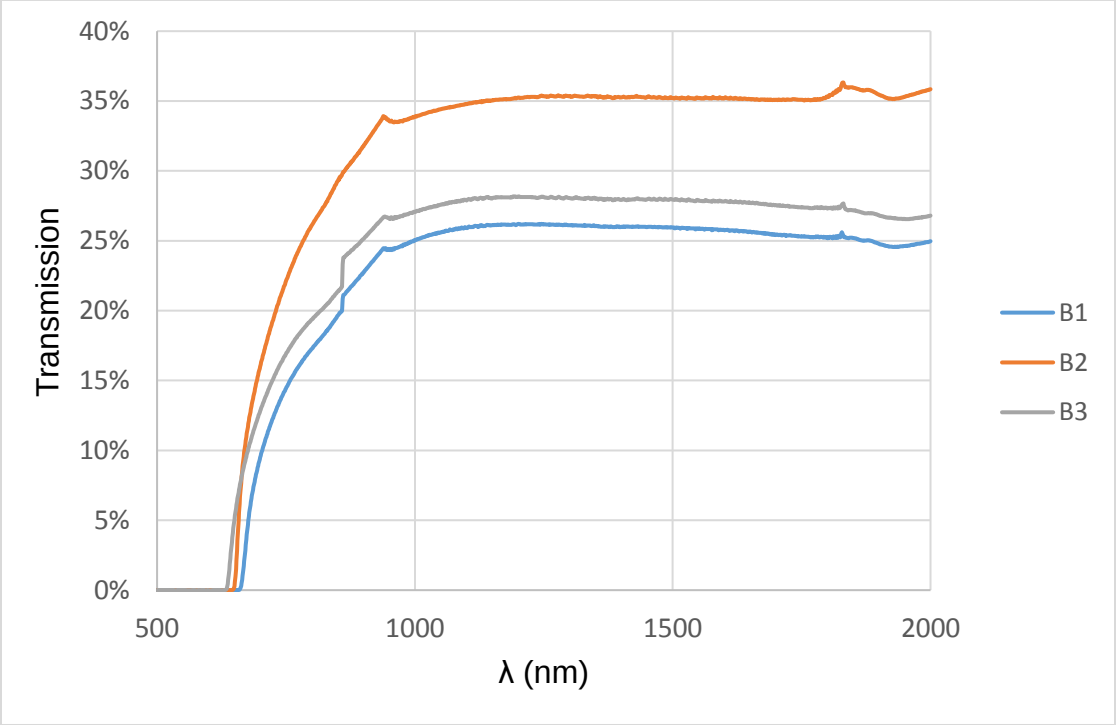

Figure 9. Band-gaps of three separate InGaP crystals

Detector

The detector used in the experiments was a ThorLabs PDA36A Si switchable gain detector which operated between 350-1100 nm. The area on the detector is 13 mm^2. The detector is shown in Figure 10. This detector was connected to a computer and monitored

with StarLab 3.20 software. This software gave an energy value in joules from each laser pulse. It also allowed multiple pulses to be averaged to help reduce the uncertainty from pulse to pulse variations.

Figure 10. ThorLabs PDA36A detector

Laser Source

The laser source used for this experiment was a multimode flashlamp pumped Nd:YAG laser operating at 1064 nm. The laser was a BrilliantA laser manufactured by QUANTEL. The laser produced Q-switched pulses of 3.4ns duration at a repetition rate of 10 Hz. Figure 11 depicts a simplified image of a Nd:YAG type Q-Swithced laser. The cavity is comprised of a rear mirror with maximum reflectivity and partially reflecting output mirror. The active medium is an Nd:YAG rod optically pulse-pumped by a flash lamp. The polarizer, quarter-wave plate and the electro-optical modulator are used to block and Q-Switch the laser emission. The laser has an output of 370 mJ, though most of the energy was dumped during the experiment.

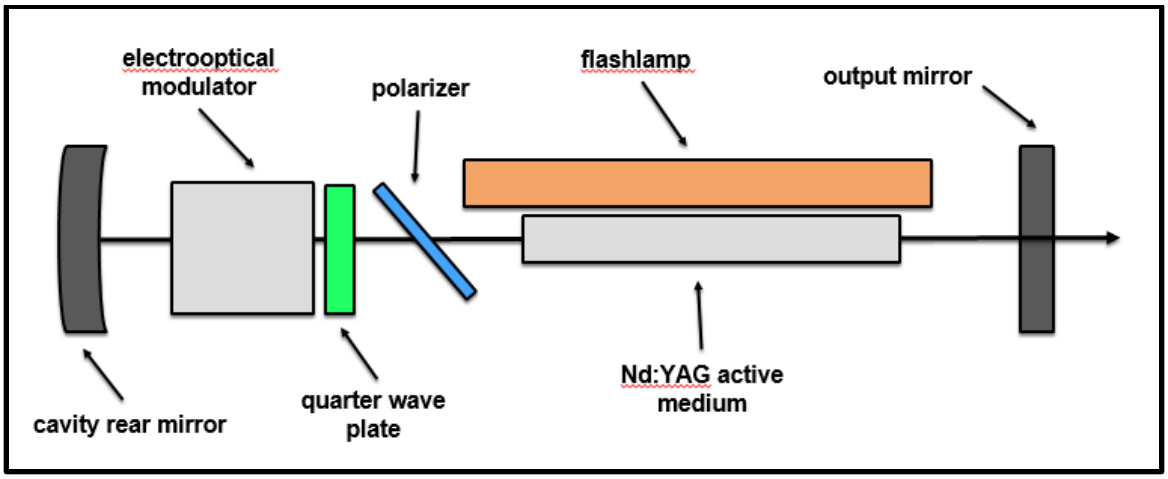

Figure 11. Simplified Diagram of Nd:YAG Q-Switched Laser

Z-Scan Experimental Setup

The Nd:YAG laser operating at 1064 nm with pulses of 3.4 ns was implemented in a Z-scan experimental setup. The Z-scan apparatus was arranged as in Figure 12. The laser energy was attenuated using a rotating waveplate/polarizer combination which allowed control over the energy in the transmitted beam. Even though the laser has an output of 370 mJ, most of the energy was dumped before reaching the sample. This was done with two separate wedges that were used in the experiment to help navigate the beam and knock down the energy of the laser. Two of the ThorLabs PDA36A Si switchable gain detectors were used in the setup. One detector was placed behind the first wedge to act as a reference detector to monitor input energy and the other was placed behind the translation stage to collect the total energy. The detectors were monitored using Starlab 3.20 software. The Gaussian output diameter of the laser was 5 mm, which was measured by burning laser alignment paper and measuring the beam size before the focusing lens. The laser light was focused down onto the samples with a 200-mm focal length lens. This gave the system an F/# of 40 and a beam spot radius of 27 μm. These

values were used to give a Rayleigh range of 2.2 mm, which is larger than the thickness of both samples, allowing the use of the thin0sample approximation. A z-translation stage was used to move the sample from approximately 20 cm in front and behind focus, in steps of 0.5 mm. After every 0.5 mm of translation, the energy was recorded of the reference detector and the detector behind the sample. The sample and the detector were translated together on the same translation stage. The Z-scan was performed on both samples with an energy of 30 μJ, and plots were made for the transmission versus z-position.

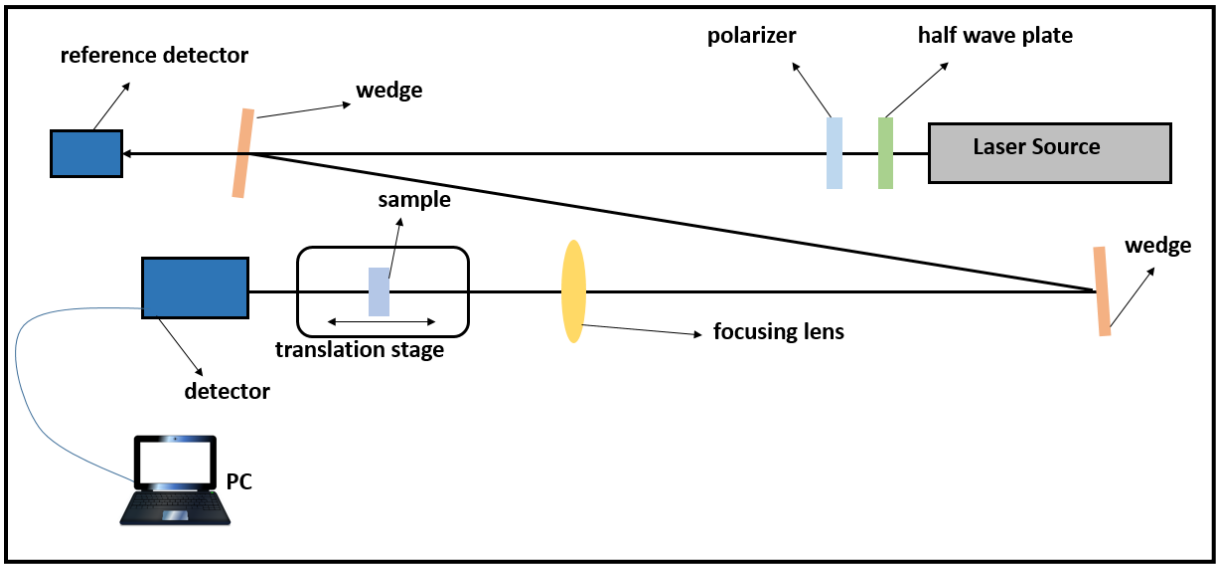

Figure 12. Z-scan experimental set-up

The detectors were used to set up a calibration before doing the experiment. This was done by rotating the half-wave plate every two degrees from the maximum energy through the minimum without any sample in the system. The energy was recorded at both detectors, and a calibration factor was found to allow the input energy to be properly monitored. The detector was also modeled as an aperture to ensure that the detector was collecting all of the transmitted light. This involved moving the detector along the x and y

axes once it was capturing all the transmitted light. If the energy did not change after moving the detector around 1 mm in all directions, it ensured the detector was collecting all the energy from the laser. The detector that was used had an area of 13 mm^2, so it was easily able to collect all the energy. The detector was placed 1 inch behind the sample. Since only nonlinear absorption was considered, the distance of the detector behind the sample did not matter as long as it was collecting all the energy from the laser.

Setting up the Z-scan was not the simplest task due to the available equipment from Raytheon and space for the experiment. This resulted in using the two separate wedges in the experimental setup, which made it more difficult to track the energy losses on the beam. Coincidentally, the alignment of the beam was more difficult and it forced careful positioning of the optics. The multiple wedges also increased the amount of scattered light picked up by the detector. There was also difficultly in creating a setup that allowed full control over the range of motion of the detector while moving it simultaneously with the sample. This was important for the detector to be adjusted in the x-direction and y-direction to make sure it was collecting all of the light. This was completed by mounting the detector on its own translation stage while having it also mounted on the same translation stage as the sample. This made it possible to move the sample and detector in all directions and able to translate the sample and detector simultaneously while taking measurements.

Another difficult task during the Z-scan experiment was accounting for the non-uniformity of the InGaP sample. The sample being non-uniform made it difficult to find the best spot on the sample to scan with the setup. This involved moving the sample in the x and y positions while it was out of focus to find a spot with the highest

transmission. Since the size of the laser illuminated on the sample changes as the z-position changes, a good spot with the sample out of focus does not necessarily mean it is a good spot on the sample at focus.

Unfortunately, the two-photon coefficient cannot be deduced from the Z-scan experiment using a nanosecond laser. This is due to the nonlinear effects of the free carriers being included. When free electrons and holes are created, they can further absorb and refract the beam, making it difficult to measure specific nonlinearities, like β. If the pulse duration is reduced, then the free-carrier effects can be neglected. A femtosecond laser should be suitable to measure the two-photon coefficient. An effective two-photon coefficient, which includes carrier and thermal, can be measured using a nanosecond laser if a different setup is used to generate a transmission versus input energy graph. This is discussed in the next section.

I-Scan Experimental Setup

The I-Scan experimental set up was similar to the Z-scan setup, however the sample position was fixed. Both of the samples were kept fixed at the focus of a 200mm lens, and input energies ranging from 10 μJ to 55 μJ were collected for both materials. The reference detector in the setup monitored the input energies. Optical wedges were used to knock down the power, and the power was further adjusted using the half wave plate attenuator. Neutral density filters, which were placed before the focusing lens, were also used in the setup to obtain a wide spectrum of input energies. One detector was placed behind the first wedge to act as a reference detector to monitor input energy and the other was placed behind the translation stage to collect the total energy. The detectors

were monitored using Starlab 3.20 software. At each input energy, over 30 pulses were taken and averaged to help eliminate pulse to pulse variations. The configuration of the I-scan is shown in Figure 13.

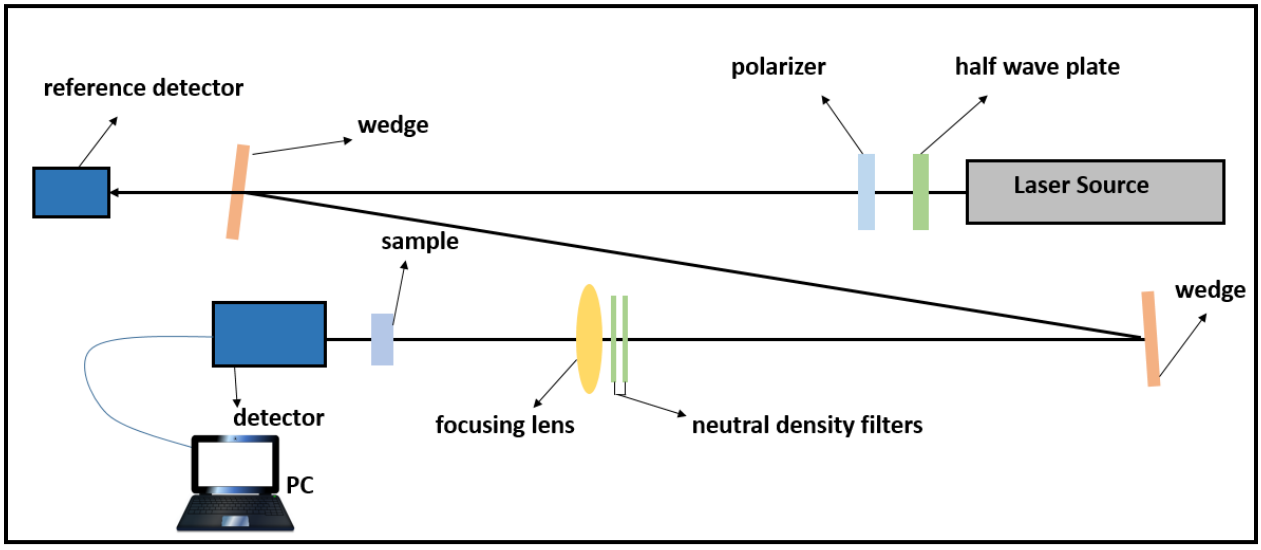

Figure 13. I-scan experimental set-up

Before taking measurements, the sample was moved along the z-axis to place the sample at focus. The lowest transmission value was found, which shows that the material is at the focus of the lens. The material was also moved along the x-axis and y-axis to find a good spot on the material. This was simple for InP since it has little non-uniformity, but for InGaP this process took time due to defects of the material. Once a spot on InGaP with high transmission was found, measurements were taken on the sample. A spot with high transmission on InGaP at focus helped eliminate the absorption of light on bad spots in the material, which was problematic during the Z-scan experiment.

The detector was placed close behind the sample to assure it was collecting all of the output energy. Since only nonlinear absorption is taken into consideration, the

distance does not affect the results as long as it is collecting the total energy. This was checked with the same process in the Z-scan setup, which involved moving the detector along the x-axis and y-axis to make sure the energy recorded by the detector was constant.

The transmission was determined over a range of intensities for both InP and InGaP and normalized by dividing out the linear losses, which was primarily from Fresnel reflections at the surfaces. The I-scan keeps the same illuminated area of light on the laser, so this helped assure that the linear losses were only from Fresnel reflections when InGaP was placed at a spot with high transmission. The pulse width was 3.4 ns, which was the full width at half maximum at 1064 nm. The 1/e pulse width for a Gaussian pulse, τ, was calculated from:

$$\tau = \frac{Pulse\ duration}{2\sqrt{\ln(2)}}. \tag{42}$$

The input irradiances were determined as,

$$I_0 = \frac{2\ \times Pulse\ Energy}{\pi {\omega_0}^2 \tau}, \tag{43}$$

with ω_0 being the beam radius at focus, defined as:

$$\omega_0 = \frac{1.27\ \lambda\ f}{2d}, \tag{44}$$

where λ is the wavelength of the laser, f is the focal length of the focusing lens, and d is the measured beam diameter before entering the lens.

A plot was made of the normalized transmittance as a function of input irradiance in GW/cm^2 for both materials. The plots were normalized to exclude the linear losses of

the materials. Plotting the irradiance versus transmittance allows for the comparison of nonlinear behavior of both materials. According to the Wherrett scaling rule, a semiconductor with a higher band-gap has a lower theoretical β value, which corresponds to a higher transmission curve compared to a semiconductor with a lower band-gap [19].

A value for β was estimated by using a fit for a pulsed Gaussian beam in time which gives the normalized transmittance by [30]:

$$T = \frac{(1-R)^2}{2q_0}\int_{-\infty}^{\infty} \ln[1 + q_0 \exp(-x^2)]\, dx, \tag{45}$$

where q_0 is defined as:

$$q_0 = \beta\left(1 - R_f\right) I_0 L_{eff}, \tag{46}$$

where I_0 is the incident irradiance, R_f is the loss due to Fresnel reflections, and L_{eff} is given by:

$$L_{eff} = \frac{1 - e^{-\alpha L}}{\alpha}, \tag{47}$$

where L is the sample thickness and α is the linear absorption coefficient. In InP, the majority of the linear losses were due to Fresnel losses so the linear absorption losses were ignored. InGaP had Fresnel losses, but it also had linear losses due to the non-uniformity of the material. If linear losses are to be ignored, Equation 47 can be simplified by making $L_{eff} = L$.

Also, the samples must be thinner than the Rayleigh range, the range over which the beam is focused. This allows for the use of thin sample approximation. The Rayleigh

range was found as 2.2 mm, which was larger than the 1 mm InP sample and 1.5 mm InGaP sample.

Once an effective β is estimated for each input irradiance and transmission measurement, a plot can be made of the effective β (cm/GW) as a function of input irradiance (GW/cm^2). For nanosecond pulses, the effective β includes the carrier and thermal effects. The estimated value for β is found by extrapolating the linear fit of the effective β graph to zero input irradiance. At zero input irradiance is where contributions from other non-linear mechanisms are insignificant.

Similarly to the Z-scan set up, there were difficulties encountered during the setup process of the I-Scan experiment. The wedges made it hard tracking the energy losses on the beam. Also, since low irradiance values are required to see the linear regime of the transmission curve, and hence extrapolate the β, a different detector must be used in the experiment. This was done by replacing the ThorLabs PDA36A Si switchable gain detector with a more sensitive silicon detector equipped with an oscilloscope. However, this detector ended up having more issues from the scattering light, particularly at lower energies. Also, since the output of the oscilloscope was in volts, being able to convert that value to energy required the creation of a calibration factor. This process was complicated because to keep the light from saturating the detector, filters had to be used to knock down the energy. This required the calibration factor to be made with the filters. In the end using this detector was abandoned due to the timing of the experiment. Using the ThorLabs PDA36A Si switchable gain was good enough to see nonlinearity of InP and InGaP, which is the primary goal of this report.

Summary

Experimental setups were constructed that tested the nonlinear performance of InGaP. InP was used as a comparison study to verify the results and experimental setup of InGaP. The experiments assembled were Z-scan and I-scan setups, and they both used the same Nd:YAG laser operating at 1064 nm and the same detectors. Both the InP and InGaP were tested using the experimental setups and the nonlinear behavior was observed. The experimental results and comparisons for InP and InGaP are presented in Chapter 4.

IV. Analysis and Results

Chapter Overview

This chapter goes through the experimental results of the semiconductors InP and InGaP using the Z-scan and I-Scan setups. InP is known to have strong nonlinear properties while they are unknown for InGaP. The nonlinear properties of InP have been well analyzed and documented in literature, which makes it an ideal candidate for testing and evaluating the experimental setups [7,24,25]. Using InP also allowed comparisons to be made to the results of InGaP. The experiments were performed in one of Raytheon's labs in El Segundo, California.

Experimental results for InP

InP was investigated using both the Z-scan and I-scan setups described in Chapter 3. InP was used as a comparison study for InGaP due to InGaP having unknown nonlinear characteristics, if any at all. Since InP is a heavily researched material, there is a lot of information on its nonlinear characteristics. If accurate results were obtained using InP in both setups, that helps validate and draw conclusions to the results of InGaP.

Data was obtained for the Z-scan setup by moving the sample with the translation stage and measuring the transmitted and reference energy at each z-position. The sample was moved over a range of 40 mm, and measurements were taken every 0.5 mm. This covered a distance which ensured that the linear and nonlinear regions were sufficiently covered. At each position, 30 laser pulses were taken and an average was recorded to help account for pulse to pulse uncertainties. The open-aperture Z-scan was performed with an input energy of 30 μJ and is shown in Figure 14.

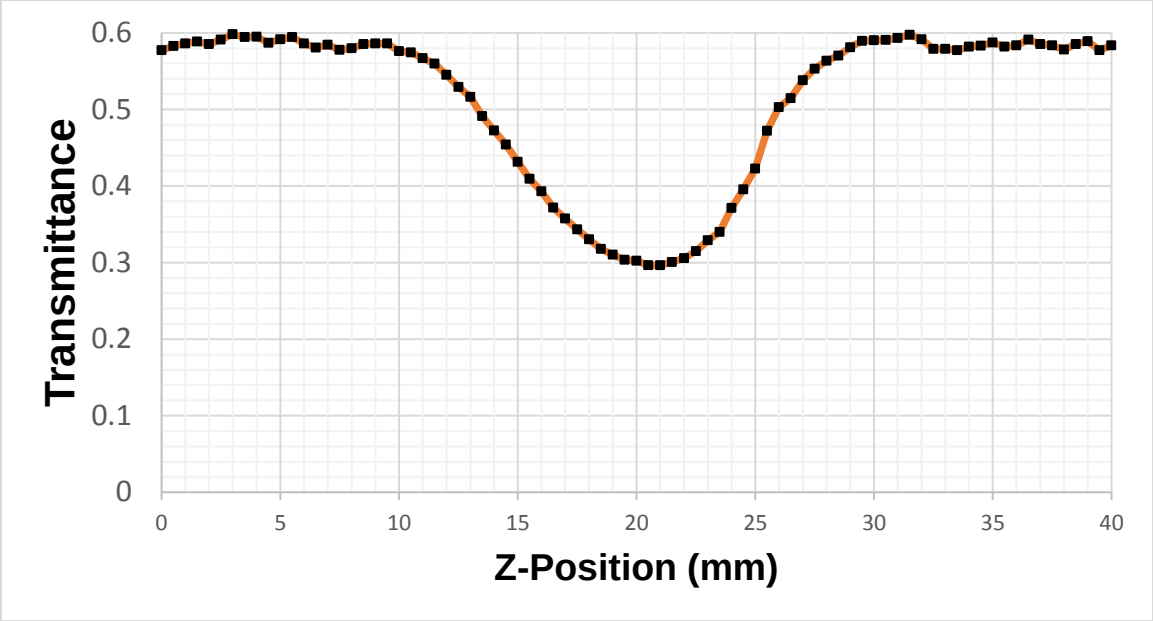

Figure 14. Open-aperture Z-scan of InP

The Rayleigh length of the focused beam for the 1mm sample was found to be 2.2 mm, which related to a beam waist at the focus of ω_0 = 27 µm. At the focus, the intensity was calculated by dividing the pulse energy by the product of the pulse length (3.4 ns) and the cross-sectional area at the focus. This gave a value for the intensity at the focus which was 0.418 GW/cm^2. The Z-scan graph demonstrated predictable nonlinear behavior for InP. The linear regime had transmission values around 0.58, which was predicted when accounting for the Fresnel losses in the sample.

For the I-Scan experimental setup, data was obtained by varying the input energy and keeping the sample fixed at the focus. The input energy was monitored using the reference detector and the transmission was determined over a range of irradiances. Similar to the Z-scan experiment on InP, 30 pulses were taken for each data point and averaged to reduce error. The results are shown in Figure 15.

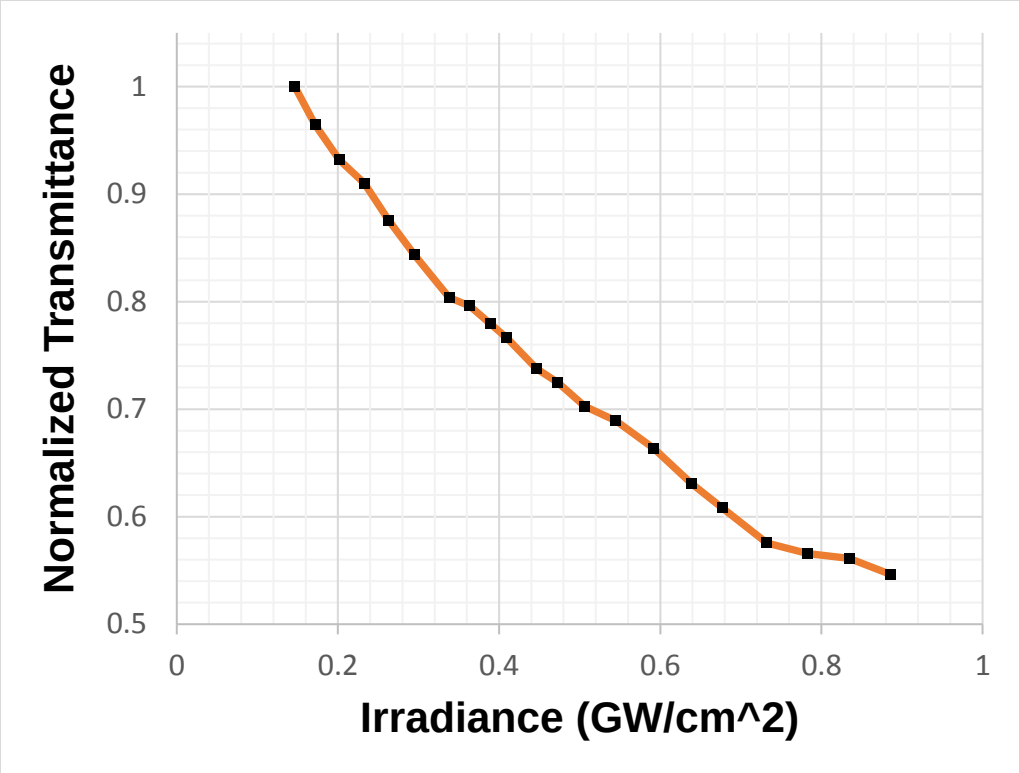

Figure 15. Nonlinear Transmittance of InP

As shown in Figure 15, InP demonstrates predicted nonlinear behavior. As the input energy increased, there was a drop off in transmission through the sample. This is an important characteristic of nonlinear behavior, as the increasing input energy leads to more two-photon absorption. The greater the incident intensity, the more photons that are incident on the sample in a given area. That is why at higher input irradiances, more two-photon absorption could occur so more free carriers were produced. The input irradiances that were recorded were not low enough to show the linear regime of the material, which made it difficult to extrapolate a β value for zero input irradiance. This was due to the dynamic range of the detector. The lowest energy values that were recorded were around 10 µJ. To get to the linear regime of the graph, input energy values around 0.1 µJ would

be required. Even though a β could not be determined, this graph helps confirm the predicted nonlinear behavior of InP.

Experimental results for InGaP

Using the same Z-scan and I-scan setups as for InP, the unknown nonlinear material InGaP was investigated. The range for the Z-scan was 50 mm and measurements were taken every 0.5 mm. This range ensured that linear and nonlinear regimes were both shown in the graph. The sample was probed out of focus before taking any measurements to find a spot of high transmission on the sample. This helped ensure that measurements were being taken in an area on the sample with less non-uniformity. The open aperture Z-scan was performed on InGaP with an input energy of 30 μJ and is shown in Figure 16.

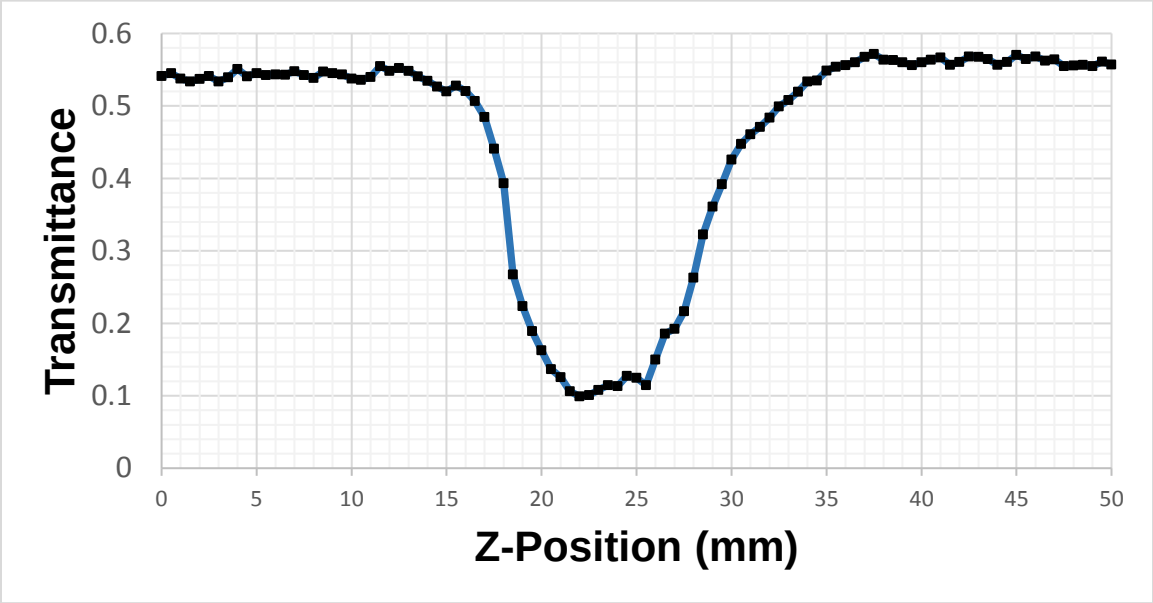

Figure 16. Open-aperture Z-scan of InGaP

The Rayleigh length of the focused beam for the 1.5mm sample was 2.2 mm, which related to a beam waist at the focus of ω_0 = 27 μm. At the focus, the irradiance was calculated by dividing the pulse energy by the product of the pulse length (3.4 ns)

and the cross sectional area at the focus. This gave a value for the irradiance at the focus which was 0.418 GW/cm^2. Similarly to InP, the InGaP sample having decreased transmission values as the sample moved towards the focus is a sign of nonlinear behavior. The linear regime of the graph had transmission values around 0.55. This value is from the linear absorption losses and Fresnel losses in the sample. The transmittance value at focus was around 0.11. This value being much lower than InP was from more light being absorbed at the focus due to material defects. As the sample was moved towards the focus of the lens, more light would catch a bad spot of the sample and allow less light to be transmitted. This was not noticeable outside of focus, as transmittance outside of focus had values similar to InP. Since the laser was illuminating a larger area of the sample, the small bad spots of the sample did not affect the overall transmittance as much compared to the sample at focus. The distortion at the position Z = 25 was most likely due to the sample translating in the x-axis or y-axis as it was being translated along the z-axis.

For the I-Scan experimental setup, data was obtained by varying the input energy and keeping InGaP fixed at the focus. The input energy was monitored using the reference detector and the transmission was determined over a range of input irradiances. The range of input irradiances corresponded to the range of input energies from 10-55 μJ. Similar to the I-scan experiment on InP, 30 pulses were taken for each data point and averaged to reduce error. The results are shown in Figure 17.

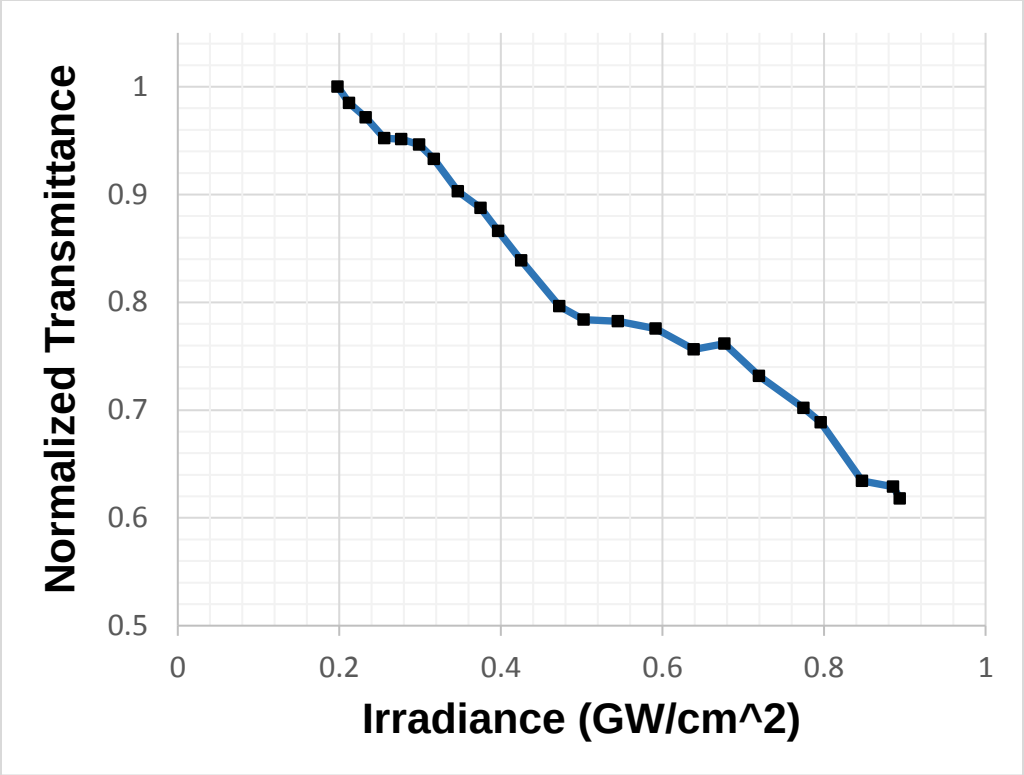

Figure 17. Nonlinear Transmittance of InGaP

As shown in Figure 17, InGaP demonstrates nonlinear behavior. As the input energy increases, there is a drop in transmission through the sample. This is because the greater the incident irradiance, the more photons that are incident on the sample in a given area coincide with more two-photon absorption. As with InP, the input irradiances that were recorded were not low enough to show the linear regime of the material, which made it difficult to extrapolate a β value for zero input irradiance. Even though a β could not be determined, this graph helps confirm that InGaP demonstrates nonlinear behavior.

Comparison of InGaP and InP

A Z-scan and I-scan experiments are constructed for the materials InP and InGaP. For all the experiments, 30 measurements were taken for each data point to improve the

signal-to-noise ratio and decrease the error of the measurements. The exact same setups were used to test both materials.

Nonlinear behavior in InP has been well researched in literature, so the nonlinear behavior found in InP was expected. The nonlinear properties of InGaP have not been researched, so the experiments on InP were used to compare and validate the results of InGaP. Both of the materials demonstrated nonlinear behavior. The open-aperture Z-scan was performed on InGaP with an input energy of 30 μJ and was performed on InP with an input energy of 30 μJ. The Z-scan graphs for both InP and InGaP demonstrated nonlinear behavior. InGaP had a transmission drop of 80% at focus, and InP had a transmission drop of 50%. Both of these materials exhibited a transmission drop at the focus due to nonlinear absorption. InGaP had a higher transmission drop at the focus compared to InP due to transmission non-uniformity throughout the sample. The growing process for InGaP is vastly more complex, which results in more defects in the material. The linear regime for InP had transmission values around 0.58, while it had values of 0.55 for InGaP. Both of these materials also have linear losses from Fresnel reflections on the surfaces of the materials.

Nonlinear behavior for both materials was also observed in the I-Scan results. Figure 18 shows the I-Scan results for both InP and InGaP.

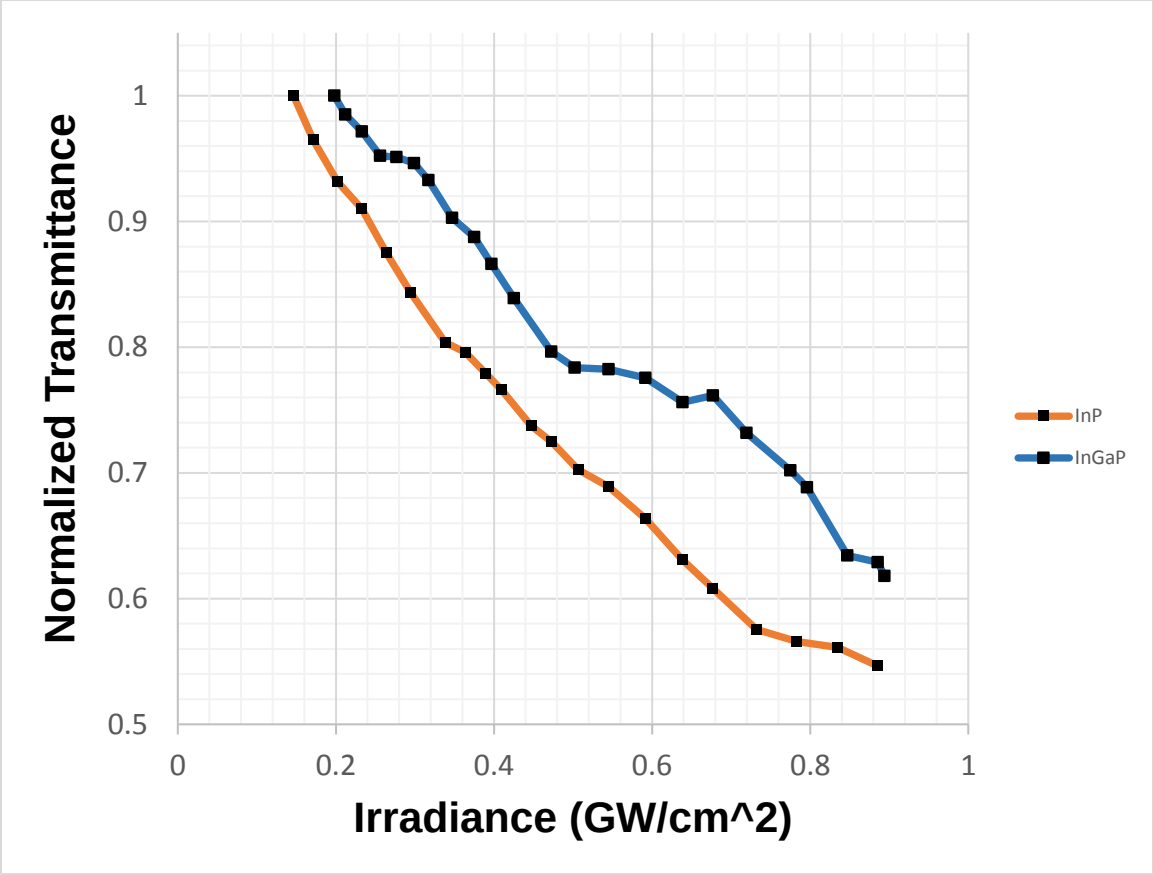

Figure 18. Nonlinear Transmittance of InP and InGaP

The results show how the transmission measurements for InP are lower than those of InGaP for the same energy. This result makes sense when considering the band-gaps and theoretical two-photon coefficients of both materials. InP has a smaller band-gap (1.34 eV) than InGaP (1.77 eV). The scaling rule, developed by Wherrett for two-photon absorption, was discussed in Chapter 2 and shows how a smaller band-gap leads to a higher theoretical two-photon absorption coefficient. So theoretically, InGaP should have a smaller β value and higher transmission curve than InP. In Chapter 2 it was discussed how materials with lower theoretical β values tend to have higher transmission verses irradiance curves, which is displayed in these results. The difference in transmission for

the same input irradiance for both samples agrees with their difference in band-gap. This confirms that InGaP has predicable nonlinearity when considering its band-gap compared with InP's band-gap. The linear portion of both materials could not be included on the graph due to the input energy required being below the noise floor of the detector. As a result, an estimated β could not compared for the materials.

Summary

Nonlinear performance on InGaP was tested by using the Z-scan and I-scan techniques. InP, which has known nonlinear behavior, was tested in addition to InGaP to validate the experimental setups and allow for comparisons to be made to the results of the unknown material. Nonlinear behavior was found for InP, which was expected. Nonlinear behavior was also found in InGaP, the unknown material. The results of both materials were presented and compared.

V. Conclusions and Recommendations

Conclusions of Research

The theory of the nonlinear processes that occur in matter were investigated for the semiconductors Indium Phosphide (InP) and Indium Gallium Phosphide (InGaP). The Z-scan and I-scan methods were chosen to explore the nonlinear properties of the materials. InGaP has unknown nonlinear properties while the nonlinear properties of InP have been well documented in research. InP was studied to verify the experimental setups and to draw conclusions for the results of InGaP.

The Z-scan and I-scan techniques which were analyzed in detail were both implemented in setups with the aim of determining the nonlinear performance of InGaP. The setups were constructed and systematically improved in order to perform repeatable measurements. Numerous measurements on both materials showed the effectiveness of the setups in determining nonlinear performance. Based on the results, nonlinear performance was found in the materials InP and InGaP. The nonlinear properties of InP that were found were expected based on literature values. InGaP also showed signs of nonlinear behavior, similar to InP. Since InP is considered a “gold standard” of nonlinear materials, the results of InGaP showing similar signs of nonlinear behavior shows the potential it has as a nonlinear material. The Z-scan results show InP had a transmission drop at focus of 50% while InGaP had a transmission drop at focus of 80%. The larger drop of transmission at focus for InGaP was due to transmission non-uniformity throughout the sample. The I-scan results showed signs of nonlinear behavior in both materials, and the results showed predictable nonlinear behavior in InGaP compared to InP when considering both of the materials’ band-gap.

The I-Scan experimental setup ended up not being sensitive enough to deduce a two-photon coefficient for the materials. This was due to the sensitivity of the detector used and an interest of time. Even though there was no two-photon coefficient found from the experiment, the results identified InGaP as a nonlinear material for the application at hand. InGaP had no prior literature research on its nonlinear properties, so the results showing strong signs of nonlinear behavior are extremely promising.

Recommendations for Future Research

Future work on the setups should include making the setups more sensitive so they are capable of finding the nonlinear coefficients of InGaP. If a more sensitive detector is used, the linear regime of the transmission as a function of input energy can be viewed and a two-photon coefficient can be found by extrapolating the input irradiance to zero. This can be done by using a silicon detector instead of the PDA36A Si switchable gain detector. The experiments could also be improved by eliminating light scatter, which was problematic when taking measurements at very low energy levels. Black tubing, draping, and fewer optical wedges in the experiment can be used to help eliminate the light scatter. Another lens with a small focal length can be placed after the sample with black tubing to focus it down onto the detector for a better method of collecting the total energy without light scatter. A top-hat spatial filter can be placed before the focusing lens to make the beam more Gaussian and dump excess energy. This would make it possible to take out the optical wedges in the experiment and help clean up the beam. With spatial filtering, the M^2 value should be closer to a TEM_{00} (Gaussian) laser beam. Also, a beam camera can be used in conjunction with software to profile the beam throughout the

waist. This would yield an experimental spot size and M^2 value. An experimental M^2 value will show the percentage of error for the experiment since it shows how close the beam is to a Gaussian laser beam. These changes to the experiment could not be completed due to the lack of time. The research team understands the path forward and plans to implement the necessary changes in the near future.

The open aperture Z-scan was used to verify InGaP had nonlinear behavior, but in future research, the open aperture Z-scan could be tested again in conjunction with a closed aperture Z-scan. These tests can be used to find more nonlinear coefficients of InGaP, including the nonlinear refraction properties of the material. Two detectors can be used in the setup so both the closed and open aperture measurements can be made simultaneously, which will help reduce the experimental errors of the experiment. The Z-scan experiment can also be done at lower input energies if scattering light is eliminated. This would produce more accurate nonlinear absorption results since a lower input energy is desired. At higher input energies, there are more unwanted thermal effects, so it is preferred to "tickle" the materials just enough to see nonlinear behavior. Additionally, a femtosecond laser can be used instead of a nanosecond laser. This will allow for a two-photon coefficient to be deduced from the Z-scan experiment. A nanosecond laser is not fast enough to obtain an accurate two-photon coefficient using the Z-Scan, but a femtosecond laser would overcome this issue.

Bibliography

[1] T. Boggess, A. Smirl, S. Moss, I. Boyd, and E. Van Stryland. Optical limiting in GaAs. IEEE Journal of Quantum Electronics, 21(5), (1985)

[2] A. Villeneuve, C. C. Yang, G. I. Stegeman, C. N. Ironside, G. Scelsi, and R. M. Osgood. Nonlinear absorption in a GaAs waveguide just above half the band-gap. IEEE Journal of Quantum Electronics, 30(5), (May 1994)

[3] K. L. Vodopyanov, O. Levi, P. S. Kuo, T. J. Pinguet, J. S. Harris, M. M. Fejer, B. Gerard, L. Becouarn, and E. Lallier. Optical parametric oscillation in quasi-phase-matched GaAs. Optics Letters, 29(16), (2004)

[4] B. Pati, E. D. Park, K. Stebbins. "Compact, passively Q-switched 523-nm laser," 2015 Conference on lasers and Electro-Optics (CLEO), San Jose, CA, (2015)

[5] D.A.B. Miller, M.H. Mozolowski, A. Miller, S.D. Smith. "Non-linear optical effects in InSb with a c.w. CO laser," Opt. Comm. 27 p133 (1978)

[6] R. Braunstein, N. Ockman, "Optical double-photon absorption in CdS," Phys. Rev. 134 pA499 (1964)

[7] L. Gonzalez, J. M. Murray, S. Krishnamurthy, S. Guha, "Wavelength dependence of two photon and free carrier absorptions in InP," Opt Express, 17 (11), (2009)

[8] Sheik-Bahae, M.; Said, A. A.; Van Stryland, E. W. "High-sensitivity, Single-beam n_2 Measurements. Optics Letters, 14 (17), (1989)

[9] Sheik-Bahae, M.; Said, A. A.; Van Stryland, E. W.; Wei, T-H; Hagan, D.J. "Sensitive Measurement of Optical Nonlinearities Using a Single Beam," IEEE Journal of Quantum Electronics, 26(4), (1990)

[10] B. Taheri, H. Liu, B. Jassemnejad, D. Appling, R. C. Powell, J. J. Song. "Intensity scan and two photon absorption and nonlinear refraction of C60 in toluene", Appl. Phys. Lett., 68, 1317 (1996)

[11] Boyd, R.W. (1992). "Nonlinear Optics," Chapter 2. Academic Press, London. Accessed 08 March 2017.

[12] Milonni P.W. and Eberly J.H. (1988). "Lasers", Chapters 2, 8, 14, 17, 18. John Wiley and Sons, New York. Accessed 10 April 2017.

[13] R. Braunstein, "Nonlinear optical effects," Phys. Rev. 125 p475 (1962)

[14] M. Göppert-Mayer. “Elementary processes with two quantum transitions,” Annalen der Physik, 18(7-8):466-479, (2009)
[15] E. Garmire. ”Resonant optical nonlinearities in semiconductors,” IEEE Journal of Selected Topics in Quantum Electronics, 6(6):1094-1110, (2000)
[16] W. Kaiser and C. G. B. Garrett. “Two-photon excitation in CaF_2:Eu^{2+},” Physical Review Letters, 7(6):229, (1961)
[17] V Nathan, A. H. Guenther, and S. S. Mitra. “Review of multiphoton absorption in crystalline solids,” Journal of the Optical Society of America B, 2(2):294-316, (1985)
[18] B. S. Wherrett. “Scaling rules for multiphoton interband absorption in semiconductors,” Journal of the Optical Society of America B, 1(1):67-72, (1984)
[19] E. W. Van Stryland, S. Guha, H. Vanherzeele, M. A. Woodall, M. J. Soileau, and B. S. Wherrett. “Verifcation of the scaling rule for two-photon absorption in semiconductors,” Journal of Modern Optics, 33:381-386, (1986)
[20] A.A. Said, M. Sheik-Bahae, D.J. Hagen, T.H. Wei, J. Wang, J. Young, E.W. Van Stryland, “Determination of bound-electronic and free-carrier nonlinearities in ZnSe, GaAs, CdTe and ZnTe.” J. Opt. Soc. Am. B 9, 405-414 (1992)
[21] J. M. Gregory, “Effect of electron and phoyon excitation of the optical properties of indirect gap semiconductors,” master’s thesis, Vanderbilt University, May 2013.
[22] I. Khoo, S. Webster, S. Kuba, Systhesis and characterization of the multi-photon absorption and excited state properties of a neat liquid 4-propyl 4-butyl diphenyl acetylene,” J. Mater. Chem., 19, 7525 (2009)
[23] A. Thiel, H. Koelsch, “Studien über das Indium,” Z. Anorg. Chem. 66 p288 (1910)
[24] Ioffe Physical-Technical Institute.
http://www.ioffe.ru/SVA/NSM/Semicond/InP.html Accessed 20 April 2017.
[25] M. Decker, R. Zhao, C. M. Soukoulis, S. Linden, M Wegener. “Twisted split-ring-resonator photonic metamaterial with huge optical cavity,” Optics Letters, 35 (10), (2010)
[26] M Sheik-Bahae, A. A. Said, T.H. Wei, D J. Hagan and E.W. Van Stryland. “Sensitive measurement of optical non-linearities using a single beam,” IEEE J. Quantum Electron. Vol 26, 760-769, (1990)

[27] C.C. Fan and H. Y. Fan. “Two-photon absorption with excitation effect for degenerate valence bands,” Phys. Rev B 9, 3502, (April 1974)

[28] Ioffe Physical-Technical Institute. http://www.ioffe.ru/SVA/NSM/Semicond/GaInP/optic.html. Accessed 15 May 2017.

[29] “Gallium Indium Phosphide – GaInP Semiconductors” AZO Materials. Accessed 15 March 2017.

[30] Sutherland, Richard L. (2003). “Handbook of Nonlinear Optics”, Chapter 9. Marcel Dekker, Inc., New York. Accessed 14 April 2017.

REPORT DOCUMENTATION PAGE

Form Approved
OMB No. 0704-0188

1. REPORT DATE *(DD-MM-YYYY)*	**2. REPORT TYPE**	**3. DATES COVERED** *(From - To)*
06-15-2017	Master's Thesis	Sept 2015 – June 2017

4. TITLE AND SUBTITLE

Measuring the Nonlinear Performance of Indium Gallium Phosphide Using the Z-Scan and Intensity Variation Methods

5a. CONTRACT NUMBER

5b. GRANT NUMBER

5c. PROGRAM ELEMENT NUMBER

6. AUTHOR(S)

Wilson, Jacob A

5d. PROJECT NUMBER

5e. TASK NUMBER

5f. WORK UNIT NUMBER

7. PERFORMING ORGANIZATION NAME(S) AND ADDRESS(ES)

Air Force Institute of Technology
Graduate School of Engineering Physics(AFIT/ENP)
2950 Hobson Way
Wright-Patterson AFB OH 45433-7765

8. PERFORMING ORGANIZATION REPORT NUMBER

AFIT-ENP-MS-17-J-013

9. SPONSORING / MONITORING AGENCY NAME(S) AND ADDRESS(ES)

Raytheon Space and Airborne System
2000 E El Segundo Blvd
El Segundo CA 90245

10. SPONSOR/MONITOR'S ACRONYM(S)

11. SPONSOR/MONITOR'S REPORT NUMBER(S)

12. DISTRIBUTION / AVAILABILITY STATEMENT

DISTRIBUTION A

13. SUPPLEMENTARY NOTES

14. ABSTRACT

Due to the increasing complexity of electronic and optical applications, there is a strong need for more customization of nonlinear materials. This thesis investigates the nonlinear performance on the tunable semiconductor, indium gallium phosphide. Indium gallium phosphide's band-gap can be customized as it is a tunable material compared to most nonlinear materials, which have fixed band-gaps. The nonlinear characteristics of indium gallium phosphide are unknown, so the well-researched nonlinear material indium phosphide is used as a comparison. Research performed in this document demonstrates two common methods that determine the nonlinear properties of a material. These methods include the Z-scan and an intensity variation scan. Indium phosphide shows expected nonlinear behavior, which verifies the methodology used in the research. Indium gallium phosphide also shows signs of nonlinear behavior. Discussion in the report provides a comparison of the nonlinear performance of the two materials, and provides insight on future experimentation on indium gallium phosphide.

15. SUBJECT TERMS

Nonlinear Optics

16. SECURITY CLASSIFICATION OF:			**17. LIMITATION OF ABSTRACT**	**18. NUMBER OF PAGES**	**19a. NAME OF RESPONSIBLE PERSON**
a. REPORT	**b. ABSTRACT**	**c. THIS PAGE**			Dr. Michael Marciniak, AFIT/ENP
U	U	U	UU	63	**19b. TELEPHONE NUMBER** *(include area code)* (937)-255-3636 x4529